ACS APPLIED MATERIALS & INTERFACES

Research Article

www.acsami.org

Next-Generation Polymer-Electrolyte-Membrane Fuel Cells Using Titanium Foam as Gas Diffusion Layer

Hyelim Choi,[⊥,†] Ok-Hee Kim,[‡,§,†] Minhyoung Kim,[‡,§] Heeman Choe,[⊥] Yong-Hun Cho,*[,⊥] and Yung-Eun Sung*[,‡,§]

[‡]School of Chemical and Biological Engineering, Seoul National University, Seoul 151-742, Republic of Korea

[§]Center for Nanoparticle Research, Institute for Basic Science (IBS), Seoul 151-742 Republic of Korea

[⊥]School of Advanced Materials Engineering, Kookmin University, Seoul 136-702, Republic of Korea

Supporting Information

ABSTRACT: In spite of their high conversion efficiency and no emission of greenhouse gases, polymer electrolyte membrane fuel cells (PEMFCs) suffer from prohibitively high cost and insufficient life-span of their core component system, the membrane electrode assembly (MEA). In this paper, we are proposing Ti foam as a promising alternative electrode material in the MEA. Indeed, it showed a current density of 462 mA cm^{-2}, being ca. 166% higher than that with the baseline Toray 060 gas diffusion layer (GDL) (278 mA cm^{-2}) with 200 ccm oxygen supply at 0.7 V, when used as the anode GDL, because of its unique three-dimensional strut structure promoting highly efficient catalytic reactions. Furthermore, it exhibits superior corrosion resistance with almost no thickness and weight changes in the accelerated corrosion test, as opposed to considerable reductions in the weight and thickness of the conventional GDL. We believe that this paper suggests profound implications in the commercialization of PEMFCs, because the metallic Ti foam provides a longer-term reliability and chemical stability, which can reduce the loss of Pt catalyst and, hence, the cost of PEMFCs.

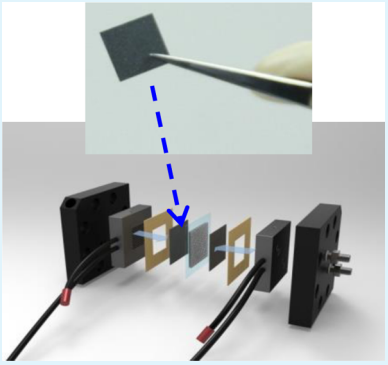

KEYWORDS: *titanium, fuel cells, MEA, foam, electrode, freeze-casting*

1. INTRODUCTION

Metallic foams are very attractive materials for advanced structural applications, because they are lightweight yet sufficiently strong to support high external loads, particularly when used as the core in sandwich structures.[1,2] These materials have recently attracted significant attention for their use in functional applications such as substrates for catalytic reactions, heat exchangers, sound absorbers, etc., because of their high specific surface area.[3,4] To obtain a porous structure with a high specific surface area for energy or functional applications, nearly all previous systems have employed ceramic or organic porous materials; very few systems have utilized metallic porous materials.[5−7] Furthermore, in an effort to fabricate porous materials with precisely controlled pore size, alignment, and density, very few successful experiments have been reported to date.[2,8,9] Freeze-casting may be a promising option for fabricating porous metallic structures with aligned and controlled pores, which can then be used as a functional material component in a number of industrial energy fields. The freeze-casting method is based on a simple principle that the metallic particles in the suspension are transferred from the moving ice-crystal-solidification front and accumulate between the ice crystals in a manner similar to salt or biological organisms trapped in the brine channels of sea ice.[10] Subsequent solidification results in both controlled nano- and micropores being formed upon adequate heat treatment.[10] Herein, we demonstrate that this freeze-casting process developed for Ti foams can be adapted to the fabrication of Ti metallic electrodes; we also report their promising potential for use as electrodes in fuel cells. In particular, we applied the freeze-cast Ti foam as an anode gas diffusion layer (GDL) to the polymer electrolyte membrane fuel cell (PEMFC), which is currently attracting considerable attention as an excellent power generator for future applications. Despite their high conversion efficiency, low operating temperature, and lack of greenhouse gas emission, there are two challenging barriers that need to be overcome before PEMFCs could be commercialized: prohibitively high costs and an insufficient life-span and reliability of the membrane electrode assembly (MEA), a core component of the PEMFCs.[11−13] The reliability of the membrane electrode assembly (MEA) is also becoming increasingly important, because present-day PEMFC stacks are employing low-cost metallic bipolar plates to be substituted for the expensive graphite bipolar plates. In this case, the MEAs and metallic bipolar plates must be held together tightly under sufficiently high compressive loads, which prevents gas leakage, reduces the contact resistance, and ensures enhanced electrical conductivity and cell performance.[14] Conventional carbon-based GDLs are

Received: February 15, 2014
Accepted: April 23, 2014
Published: April 23, 2014

   dx.doi.org/10.1021/am500962h | ACS Appl. Mater. Interfaces 2014, 6, 7665−7671

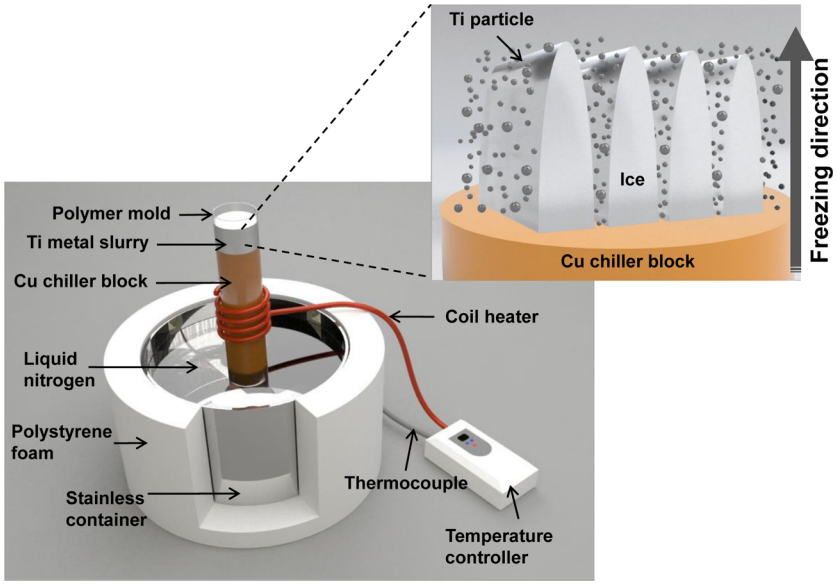

Figure 1. Schematic diagram of the freeze-casting apparatus used in this study and the growth process of ice crystals during freeze-casting.

highly sensitive to clamping pressure, because they can easily be jammed in the gas flow channels and be damaged at high clamping loads. Moreover, the permeability and porosity of the GDL decrease, and thus, reactants and products move sluggishly in the gas flow channels; as a consequence, the cell performance degrades dramatically.[15,16] We believe that the Ti foam can help resolve these issues and be a promising material candidate for highly efficient and reliable GDL electrodes, because Ti possesses desirable ductility and fracture toughness, as well as excellent corrosion resistance, which is expected to lead to prolonged life-span reliability of the MEAs.[17,18] In this context, the present study assesses the single-cell performance of the MEAs using freeze-cast Ti foam as anode GDLs and compares the results to those of the conventional carbon-based GDLs. This paper further discusses the profound implications of using freeze-cast metallic foam as an electrode in the PEMFC and its other potential applications in similar energy fields.

2. EXPERIMENTAL PROCEDURES

Ti foam was selected as a model foam material in this study and was fabricated by a freeze-casting process (Figure 1). Ti powder (Alfa Aesar, MA, USA) composed of 325 mesh-sized particles was used for all experiments. Prior to freeze-casting, 0.28 g of poly(vinyl alcohol) (PVA, M_w 89,000−98,000, purity ∼99%, Sigma-Aldrich Co., MO, USA) was dissolved in 10 mL of distilled water, and 11.25 g of Ti powder was added to the prepared solution to complete the slurry. The slurry was then poured directly onto the top of the Cu chiller rod standing in the stainless steel vessel under liquid N_2. The frozen green-body was lyophilized to remove ice through sublimation at −90 °C and at 5×10^{-3} Torr for ∼20 h (Freeze-dryer, Operon, OPR-FDU-7003, Republic of Korea). The lyophilized green-body was then sintered in a vacuum furnace via a two-step heat-treatment process: at 300 °C for 3 h and then at 1100 °C for 7 h.

To evaluate the electrochemical performance of the MEA with the fabricated Ti foam as the anode GDL, a typical MEA fabrication method was used (Figure 2). In particular, a catalyst ink was prepared using a carbon-supported Pt catalyst powder (40 wt % Pt/C, Johnson Matthey) and a Nafion solution (5 wt %, Aldrich) dissolved in isopropyl alcohol (IPA, Aldrich) and deionized water. A spraying method was used to form the Pt catalyst layer on the Nafion 212 polymer electrolyte membrane (Dupont, USA), where the Pt loading

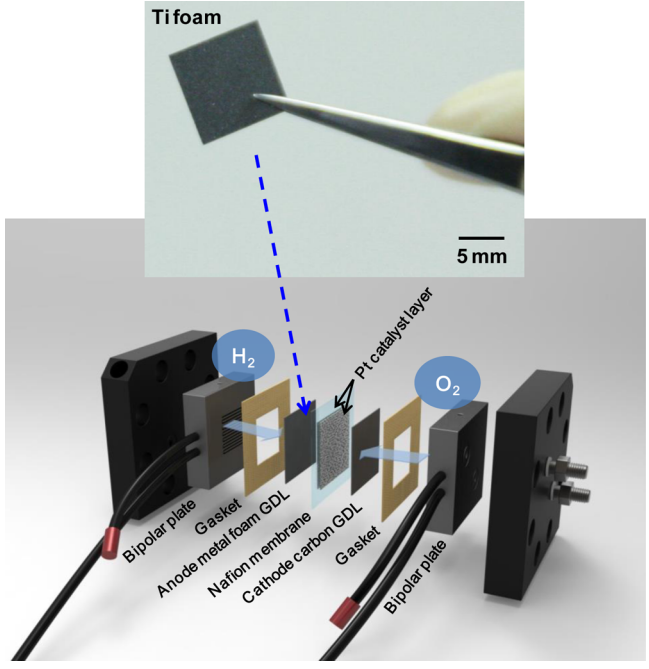

Figure 2. Schematic diagram of a typical MEA fabrication and test method with an optical micrograph of a Ti foam anode GDL sample used in this study.

was 0.2 mg cm^{-2}. The single-cell performance was evaluated and compared between the MEAs with three different GDL materials attached to the catalyst-coated membrane: the single-layered Ti foam GDL (Figure 3), GDL with a microporous layer (35BC, SGL), and GDL without a microporous layer (Toray 060, Toray). The single-cell was assembled with eight screws and using a torque wrench at the pressure of 8 N m. Fully humidified H_2 and air were supplied to the anode and cathode, respectively, during the single-cell performance evaluation. The single-cell test was carried out at 70 °C. The temperatures of the humidifiers were maintained at 75 and 70 °C at the anode and cathode, respectively, with an anode stoichiometry of 1.0, an O_2 cathode stoichiometry of 2.5, and an air stoichiometry of 2.2. These stoichiometry calculations were carried out on the basis of the measurements of flow rates and geometric area of the flow channel plate used in this study. The flow rates of H_2 and air were 150 and 800

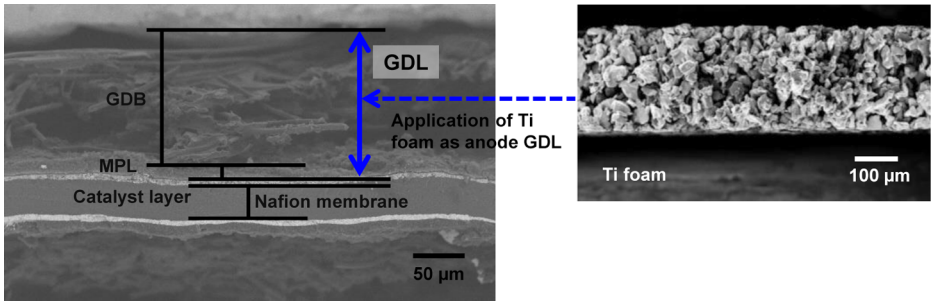

Figure 3. SEM images of a typical MEA with the conventional GDL containing both GDBL and MPL (left) and of cross-section of the single-layered Ti foam GDL (right) fabricated through freeze-casting in this study.

ccm, respectively, and all MEAs used in this study were inserted in a single cell module that had a graphite plate with a serpentine gas flow channel of 5 cm^2 geometric area. The cyclic voltammetry (CV) test was performed using a potentiostat-galvanostat system (IM6, Zahner, Germany) to estimate the electrochemical surface area (ECSA) of the assembled MEA. The potential was varied from 0.05 to 1.2 V at a scan rate of 100 mVs^{-1} by supplying humidified 50 ccm H_2 to the cathode for reference electrode and 150 ccm N_2 to the anode for working electrode, respectively. Electrochemical impedance spectroscopy (EIS) was carried out to determine the resistance of the MEA with frequencies varying from 10 kHz to 100 mHz, at a cell potential of 0.7 V with an amplitude of 5 mV.[19]

Accelerated GDL corrosion testing was performed under the same temperature and gas-flow conditions as the single-cell performance test with an external voltage of 1.45 V applied to accelerate the corrosion process. The test was performed for 72 h, during which the weight and thickness changes of the GDLs were measured to determine the extent of the corrosive deterioration. Changes in the thickness of the samples were carefully measured using an Ultra-Cal IV Electronic Digital Caliper (Ted Pella, Inc., USA). The experimentally measured digital values were also confirmed by directly reading measurements. Mass change measurements were carried out using a microbalance (Ohaus, Analytical Plus 250D). All the measurements were performed in triplicate with the mean value used for further analysis. Samples were completely dried in an oven at 60 °C prior to each measurement. The surface morphological change of the GDLs was also analyzed with SEM. Porosity and pore size distribution measurements were carried out on the Ti foam and SGL 35BC GDLs using Hg intrusion porosimetry (MIP, AutoPore IV 9510, Micromeritics).

3. RESULTS AND DISCUSSION

3.1. Material Processing and Microstructure. This study particularly used freeze-casting (Figure 1) to fabricate the Ti foam anode GDL, because this process is relatively easy to perform compared to alternative metal-foam processing techniques and is easily scalable for mass production (Figure 4a).[20] It is of particular interest to note that Ti foam samples fabricated in this study show execellent flexibility as demonstrated in Figure 4b.

The resulting microstructure generally tends to have elongated aligned pores on the order of several tens of micrometers, but we instead sought to produce Ti foams with smaller pores for two reasons: to achieve (i) a higher density of reactive surface area and (ii) better mechanical reliability in the thin foil form. This distribution of smaller pore sizes could be obtained by freezing the Ti foam green-bodies maintained at a much lower temperature on the top of the Cu chiller rod; hence, the freezing rates in the Ti foam green-bodies were much faster. This procedure was carried out using liquid N_2 as the freezing medium during the freeze-casting process. Figure 5 shows that the major distribution of pore size in the Ti foam fabricated in this study lies in the range of a few tens of

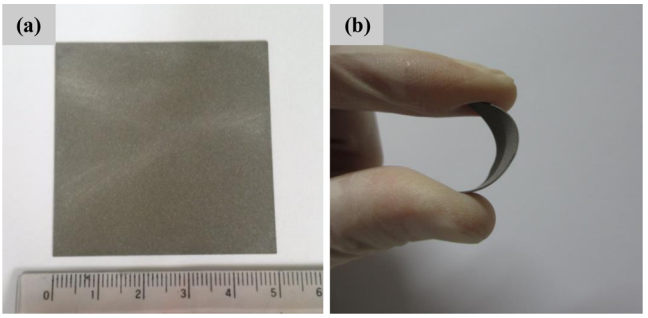

Figure 4. Optical images of (a) 5.0 × 5.0 cm^2 Ti foam GDL fabricated through freeze-casting and (b) a Ti foam sample bent by fingers to demonstrate its flexibility.

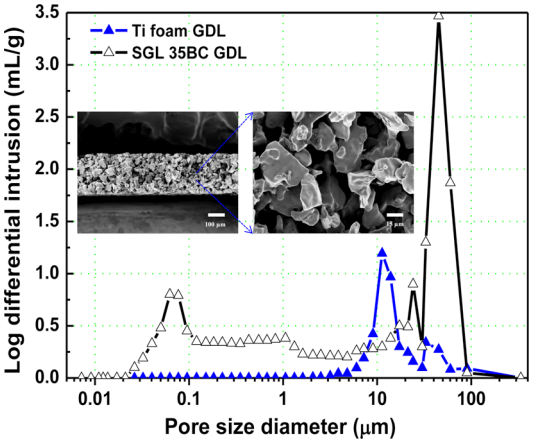

Figure 5. Pore size distribution in the Ti foam anode GDL (blue line) and conventional SGL 35BC GDL (black line) determined by MIP. Shown in the inset are SEM images of a cross-section of the Ti foam anode GDL used in this study.

micrometers, with a narrow distribution in the range of several tens of micrometers. Achieving two different size distributions for the pores appears to be desirable, because the smaller pores are advantageous for maximizing the reactive surface areas of the Ti foam and providing higher electrocatalytic activity, whereas the larger pores are expected to be more suitable for improving water and gas flows in the MEAs. On the other hand, the conventional GDL with a microporous layer (MPL, SGL 35BC) shows that the major distribution of pore size is in the range of several tens of micrometers, which is several times greater than the major distribution range of pore sizes in the Ti foam. In the conventional SGL 35BC GDL, an additional minor pore size distribution is displayed in the range of several

dx.doi.org/10.1021/am500962h | ACS Appl. Mater. Interfaces 2014, 6, 7665−7671

tens of nanometers. The larger pores originated from the gas diffusion backing layer (GDBL), which is normally a carbon-fiber-based product, whereas the smaller pores are due to the presence of the MPL composed of carbon powder and a hydrophobic agent.[21] Shown also in the inset of Figure 5 are cross-sectional SEM images of the Ti foam anode GDL. The enlarged cross-sectional SEM image shows that, owing to the fast freezing rate in the green-body of the Ti foam using liquid N_2, a firmly connected three-dimensional strut construction was obtained along with relatively smaller pores on the order of a few tens of micrometers, while sacrificing the typical elongated pore shape.[2,9]

3.2. Accelerated Corrosion Test. Carbon is reported to be corroded considerably during the operation of a fuel cell.[22] We carried out an accelerated corrosion test (ACT) and compared the corrosion resistance of Ti and carbon GDLs under the same temperature and gas-flow conditions as the single-cell performance test with an accelerated external voltage of 1.45 V. Figure 6 shows the change in the relative weight and

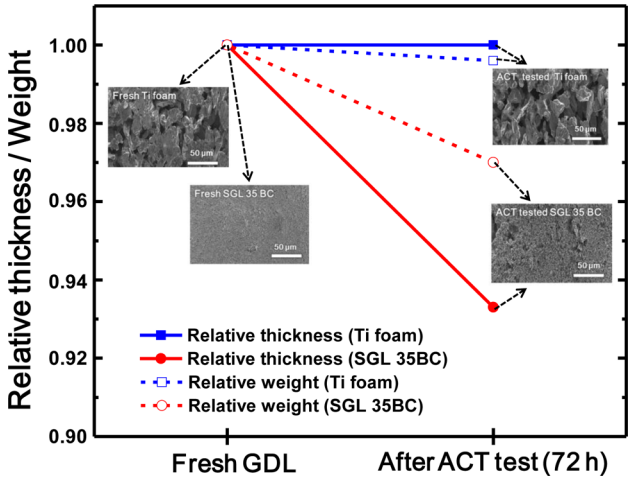

Figure 6. Changes in normalized thickness and weight and corresponding SEM images of surface morphology of the GDLs before and after ACT for 72 h.

thickness of each GDL before and after the 72 h accelerated corrosion test (ACT). While the thickness of the SGL 35BC GDL decreased by ca. 6.7% (from 300 ± 5 to 280 ± 5 μm) during the ACT, the thickness of the Ti foam GDL remained nearly the same after the test (240 ± 5 μm), which agrees well with the weight-loss comparison; while approximately 3% weight loss (from 10.88 ± 0.02 to 10.55 ± 0.02 mg) was observed in the SGL 35BC GDL after the test, the weight of the Ti foam GDL decreased by only 0.4% (from 33.85 ± 0.02 to 33.70 ± 0.02 mg). The difference in corrosion resistance between the carbon and Ti GDLs is remarkable and somewhat expected, because carbon has relatively weak corrosion resistance and is completely corroded within a few hours under that high external voltage of 1.45 V,[22] whereas Ti has inherently strong corrosion resistance due to the formation of the dense, thin TiO_2 film on the surface.[23] The change in the surface morphology of each GDL was observed to determine the effect of corrosion. As shown in Figure 6, the surface roughness of the SGL 35BC visibly increased after the test. Compared to the fresh sample, the corroded SGL 35BC showed larger and darker spots, which indicates the formation of pores on the surface because of the corrosion test. In contrast, little to no noticeable changes were observed in the surface morphology of the Ti foam GDL. Therefore, the Ti foam GDL showed superior corrosion resistance under the PEMFC on/off condition, compared to that of the conventional GDL (SGL 35BC).[22] Given that the conventional carbon-based GDL is likely to lead to performance degradation of the PEMFCs as a result of corrosion and, hence, diminish the mechanical reliability of the MEA, the Ti foam GDL can be an excellent GDL electrode replacement, because of its long-term durability under the corrosive environment of PEMFC operations.

3.3. Single-Cell Performance Test. Figure 7 displays the single-cell performance test results of the MEAs with the single-layered Ti foam anode GDL, compared to those of the MEAs with conventional carbon-based GDLs with and without an MPL (SGL 35BC and Toray 060, respectively). In Figure 7a,b, the MEA with the Ti foam anode GDL displays a significantly improved performance compared to the Toray 060 GDL, with its maximum power density reaching over 700 mW cm^{-2}. For example, with a 200 ccm O_2 supply at 0.7 V in Figure 7a, the MEA with the Ti foam anode GDL exhibits a current density of 462 mA cm^{-2}, which is approximately 166% higher than that of the Toray 060 GDL (278 mA cm^{-2}). When a 800 ccm air supply was used at 0.7 V (Figure 7b), the MEA with the Ti foam anode GDL exhibits a current density of 262 mA cm^{-2}, which is approximately 166% higher than that of Toray 060 GDL (158 mA cm^{-2}). The open-circuit voltage (OCV) measured for the MEA containing the Ti foam anode GDL is 938 mV at 70 °C, versus 928 mV for the MEA containing the conventional GDL under O_2. The OCV was determined by the mixed potential of Pt/PtO catalyst surface and H_2 crossover.[24]

Perhaps most surprisingly, the single-cell performance of the MEA with the single-layered Ti foam anode GDL is superior to that of the MEA with the SGL 35BC GDL containing an MPL, as shown in Figure 7a,b and Table 1. When 200 ccm O_2 and 800 ccm air supplies were used at 0.7 V, the MEA with the Ti foam anode GDL showed 462 and 262 mA cm^{-2}, respectively, which are significantly higher than those of the MEA with the SGL 35BC GDL (375 and 216 mA cm^{-2}, respectively). This finding is consistent with the electrochemical impedance spectroscopy (EIS) measurements obtained by operations under H_2/air supplementations, as shown in Figure 7c. The MEA with the Ti foam anode GDL exhibits a smaller semicircle compared to that of the conventional anode GDL, suggesting that the Ti foam GDL has a decreased activation loss and lower charge-transfer resistance relative to the conventional Toray 060 GDL.

Additionally, this finding also agrees well with the polarization test results in Figure 7a,b, because the impedance diameters are proportional to the polarization curve slopes at the measured cell voltage. The improved conductivity for the MEA containing the Ti foam anode GDL is attributed to its role in the composition of three-dimensionally interconnected struts, taking advantage of naturally high electrical conductivity and effective electron paths with less resistance. Moreover, the MEA containing the Ti foam anode GDL shows a more gradual slope in the high-frequency region, which indicates a lower anode-activation loss. To examine the effect of the ACT test on the impedance of the MEA containing Ti foam, EIS measurements were obtained for the Ti foam cathode GDL both before and after the ACT test by operations under H_2/air supplementations with a cell potential ranging from 0.55 to 0.80 V (Figure S1, Supporting Information), because the

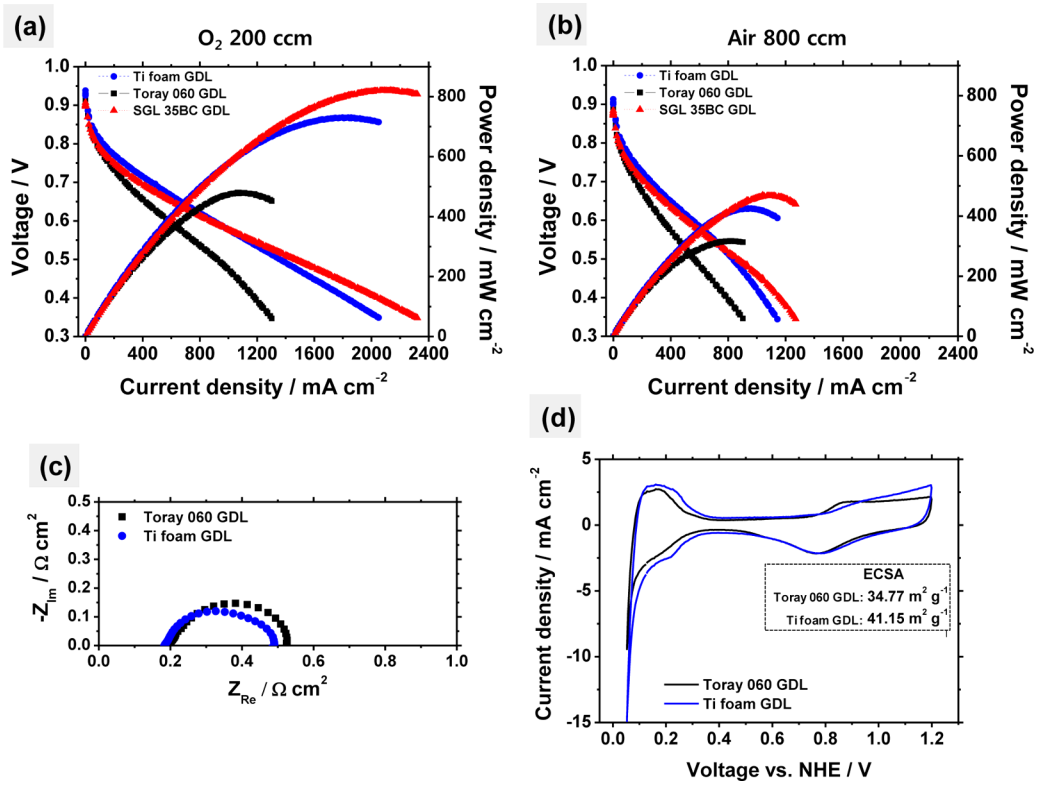

Figure 7. Comparison of MEA anode performance of the Ti foam and conventional GDLs: Single-cell polarization curves of the MEAs with the Ti-foam anode GDL and conventional GDLs with supplies of (a) 200 ccm O_2 and (b) 800 ccm air. Also shown are (c) electrochemical Nyquist impedance spectra of the Ti foam anode GDL in comparison with that of the conventional GDL and (d) cyclic voltammograms of the MEA with the Ti foam anode GDL in comparison with that of the conventional GDL.

Table 1. Summary of Single-Cell Performance of PEMFCs with MEAs, Including Ti Foam and Conventional Anode GDLs

	current density at 0.7 V (mA cm^{-2})	
material	O_2 200 ccm	air 800 ccm
Toray 060 GDL	278	158
SGL 35BC	375	216
Ti foam anode GDL	462	262

cathode region is generally more prone to corrision degradation than the anode region. Despite the superior corrosion resistance of the Ti foam GDL (Figure 6), EIS measurements show degraded performance of the MEA with the Ti foam cathode GDL, which is manifested by the shift of the semicircle to the right and its larger diameter after the ACT test. This is somewhat anticipated, because some degree of carbon corrosion and degradation in the catalyst layer also takes place during the ACT test.[25] It is therefore difficult to evaluate the effect of the ACT test on the impedance solely in the context of the corrosion resistance of Ti foam.

Figure 7d shows the cyclic voltammetry (CV) test results for the MEA with the Ti foam anode GDL, compared to those for the MEA with the conventional Toray 060 GDL. Typical H_2 adsorption/desorption peaks were observed around 0.1 V, the double-layers around 0.4 V, and O_2 redox peaks at 0.6 V in both the MEA samples. The electrochemical surface area (ECSA) of the MEA with the Ti foam anode is approximately 41 m^2g^{-1}, which is higher than that of the MEA with the conventional GDL (~35 m^2g^{-1}). This result also suggests that the Ti foam is suitable for use as an anode in PEMFCs, because it has a unique three-dimensionally connected structure with a high specific surface area to efficiently react with H_2 and O_2. Alternatively, a slightly different processing approach should be adopted for the microstructural optimization of the Ti foam GDL for use as a cathode in the MEA of the PEMFCs. The cathode tends to have a higher activation loss and a more rigorous concentration loss than the anode. Although the anode involves lighter H_2 molecules with a reduced transport resistance and a faster catalytic reaction, the cathode interacts with heavier O_2 molecules with a higher transport resistance, along with a byproduct of water molecules.[26] Therefore, Ti foams with larger and more directional porous channels should be designed for use as cathodes to guarantee the easy flow of water molecules and improve the performance. This microstructural alteration can be achieved by precisely controlling the processing parameters during the freeze-casting fabrication, e.g., changing freezing rate, slurry composition, or sintering temperature.[2,9]

The enhanced performance of the MEA with Ti foam suggests profound implications in the commercialization of PEMFCs, because the metallic Ti foam provides long-term reliability and chemical stability (Figure 6), which can reduce the loss of the Pt catalyst and the overall cost of PEMFCs. We used Ti as a model material, because it has a relatively low room-temperature resistivity of 5.4×10^{-5} Ω·cm in its bulk form, great strength and ductility, and sufficient corrosion resistance to maintain its functionality in the acidic solution of the MEAs.[22,27] In particular, metallic foam has a competitive advantage with its inherently low electrical resistivity. We did not conduct an experimental measurement for the resistivity of the Ti foam in this study, but on the basis of experimental data

dx.doi.org/10.1021/am500962h | ACS Appl. Mater. Interfaces 2014, 6, 7665−7671

showing a near linear relationship between the electrical conductivity and relative density of open-cell metallic foams,[28] the Ti foam (~66% porosity) used in this study is expected to have a room-temperature resistivity of ~3.6×10^{-4} Ω·cm, which is significantly lower than that of Toray 060 GDL (~8.0×10^{-2} Ω·cm, provided by Toray).

The choice of material, however, does not have to be limited to Ti foam only; other metallic foams with the required properties can also be used. In principle, a variety of metallic foams can be processed using freeze-casting, because the underlying theory is associated more with physical interactions, rather than with chemical transitions between the metallic particle slurry and the growth of ice crystals.[10] Most importantly, this study may be considered a fundamental framework in the context of using metallic foams as electrodes in other energy applications, because the experimental results using the Ti foam and subsequent analytical insights gained in this study could also apply to other strategic energy fields such as the electrodes in other types of fuel cells, dye-sensitized solar cells, and batteries, to name a few.[29]

4. CONCLUSION

We have demonstrated that the freeze-cast Ti foam introduced in this paper shows superior reliability and electrochemical performance and is a promising material candidate for highly efficient and reliable GDL electrodes in the MEA of the PEMFC. It showed an excellent single-cell performance, which was superior to those of the Toray 060 GDL and the SGL 35BC GDL without and with an MPL, respectively. This is attributed mainly to the unique three-dimensionally connected strut structure in the Ti metallic foam.

■ ASSOCIATED CONTENT

Ⓢ Supporting Information

Table S1: some physical properties of Ti foam along with those of traditional SGL and Toray GDLs, including the thickness, porosity, and relative density of the three different types of GDLs. Figure S1: a set of EIS tests for the MEA containing the Ti foam cathode GDL both before and after the ACT test. This material is available free of charge via the Internet at http://pubs.acs.org/.

■ AUTHOR INFORMATION

Corresponding Authors

*E-mail: yhun00@kookmin.ac.kr.

*E-mail: ysung@snu.ac.kr.

Author Contributions

†H. Choi and O.-H. Kim contributed equally to this work.

Notes

The authors declare no competing financial interest.

■ ACKNOWLEDGMENTS

This work was supported by the Institute for Basic Science (IBS) in Korea. Y.-H. Cho and H. Choe acknowledge financial support by the Priority Research Centre Program (2009-0093814) and Basic Science Research Program (2013R1A1A2061636) through NRF funded by the Ministry of Education.

■ REFERENCES

(1) Gibson, L. J.; Ashby, M. F. *Cellular Solids Structure and Properties*, 2nd ed.; Cambridge University Press: Cambridge, UK, 1997.

(2) Chino, Y.; Dunand, D. C. Directionally Freeze-Cast Titanium Foam with Aligned, Elongated Pores. *Acta Mater.* **2008**, *56*, 105−113.

(3) Banhart, J. Manufacture, Characterisation and Application of Cellular Metals and Metal Foams. *Prog. Mater. Sci.* **2001**, *46*, 559−621.

(4) Zhao, C. Y. Review on Thermal Transport in High Porosity Cellular Metal Foams with Open Cells. *Int. J. Heat Mass Transfer* **2012**, *55*, 3618−3632.

(5) Chen, H. S.; Lue, S. J.; Tung, Y. L.; Cheng, K. W.; Huang, F. Y.; Ho, K. C. Elucidation of Electrochemical Properties of Electrolyte-Impregnated Micro-Porous Ceramic Flms as Framework Supports in Dye-Sensitized Solar Cells. *J. Power Sources* **2011**, *196*, 4162−4172.

(6) Do, J.-S.; Yu, S.-H.; Cheng, S.-F. Thick-Film Nickel−Metal-Hydride Battery Based on Porous Ceramic Substrates. *J. Power Sources* **2003**, *117*, 203−211.

(7) Chen, H.; Cheng, K.; Wang, Z.; Weng, W.; Shen, G.; Du, P.; Han, G. Preparation of Porous NiO-Ce0.8Sm0.2O1.9 Ceramics for Anode-Supported Low-Temperature Solid Oxide Fuel Cells. *J. Mater. Sci. Technol.* **2010**, *26*, 523−528.

(8) Launey, M. E.; Alsem, D. H.; Saiz, E.; Tomsia, A. P.; Ritchie, R. O. Tough, Bio-Inspired Hybrid Materials. *Science* **2008**, *322*, 1516−1520.

(9) Cox, M. E.; Kecskes, L. J.; Mathaudhu, S. N.; Dunand, D. C. Amorphous Hf-Based Foams with Aligned, Elongated Pores. *Mater. Sci. Eng., A* **2012**, *533*, 124−127.

(10) Deville, S. Freeze-Casting of Porous Ceramics: A Review of Current Achievements and Issues. *Adv. Eng. Mater.* **2008**, *10*, 155−169.

(11) Carrette, L.; Friedrich, K. A.; Stimming, U. Fuel Cells: Principles, Types, Fuels, and Applications. *ChemPhysChem* **2000**, *1*, 163−193.

(12) Coutanceau, C.; Koffi, R. K.; Léger, J.-M.; Marestin, C.; Mercier, R.; Nayoze, C.; Capron, P. Development of Materials for Mini DMFC Working at Room Temperature for Portable Applications. *J. Power Source* **2006**, *160*, 334−342.

(13) Cho, Y.; Cho, Y.; Lim, J.; Park, H.; Jung, N.; Ahn, M.; Choe, H.; Sung, Y. Performance of Membrane Electrode Assemblies Using PdPt Alloy as Anode Catalysts in Polymer Electrolyte Membrane Fuel Cell. *Int. J. Hydrogen Energy* **2012**, *37*, 5884−5890.

(14) Ge, J.; Higier, A.; Liu, H. Effect of Gas Diffusion Layer Compression on PEM Fuel Cell Performance. *J. Power Sources* **2006**, *159*, 922−927.

(15) Chang, W. R.; Hwang, J. J.; Weng, F. B.; Chan, S. H. Effect of Clamping Pressure on the Performance of a PEM Fuel Cell. *J. Power Sources* **2007**, *166*, 149−154.

(16) Bazylak, A.; Sinton, D.; Liu, Z.-S.; Djilali, N. Effect of Compression on Liquid Water Transport and Microstructure of PEMFC Gas Diffusion Layers. *J. Power Sources* **2007**, *163*, 784−792.

(17) Boyer, R., Welsch, G., Collings, E. W., Eds. *Materials Properties Handbook: Titanium Alloys*; ASM International: Materials Park, OH, USA, 1998.

(18) Donachie, M. J. *Titanium: A Technical Guide*, 2nd ed.; ASM International: Materials Park, OH, USA, 2000.

(19) Lim, J. W.; Cho, Y.-H.; Ahn, M.; Chung, D. Y.; Cho, Y.-H.; Jung, N.; Kang, Y. S.; Kim, O.-H.; Lee, M. J.; Kim, M.; Sung, Y.-E. Ionic Resistance of a Cathode Catalyst Layer with Various Thicknesses by Electrochemical Impedance Spectroscopy for PEMFC Fuel Cells and Energy Conversion. *J. Electrochem. Soc.* **2012**, *159*, B378−B384.

(20) Fukasawa, T.; Deng, Z.-Y.; Ando, M.; Ohji, T.; Goto, Y. Pore Structure of Porous Ceramics Synthesized from Water Based Slurry by Freeze-Dry Process. *J. Mater.Sci.* **2001**, *36*, 2523−2527.

(21) Chun, J. H.; Park, K. T.; Jo, D. H.; Lee, J. Y.; Kim, S. G.; Lee, E. S.; Jyoung, J.-Y.; Kim, S. H. Determination of the Pore Size Distribution of Micro Porous Layer in PEMFC Using Pore Forming Agents Under Various Drying Conditions. *Int. J. Hydrogen Energy* **2010**, *35*, 11148−11153.

(22) Reiser, C. A.; Bregoli, L.; Patterson, T. W.; Yi, J. S.; Yang, J. D.; Perry, M. L.; Jarvi, T. D. A Reverse-Current Decay Mechanism for Fuel Cells. *Electrochem. Solid-State Lett.* **2005**, *8*, A273−276.

(23) Choi, M.; Hong, E.; So, J.; Song, S.; Kim, B.-S.; Yamamoto, A.; Kim, Y.-S.; Cho, J.; Choe, H. Tribological Properties of Biocompatible Ti−10W and Ti−7.5TiC−7.5W. *J. Mech. Behav. Biomed. Mater.* **2014**, *30*, 214−222.
(24) Zhang, J.; Tang, Y.; Song, C.; Zhang, J.; Wang, H. PEM Fuel Cell Open Circuit Voltage (OCV) in the Temperature Range of 23°C to 120°C. *J. Power Sources* **2006**, *163*, 532−537.
(25) Oh, H.-S.; Lim, K. H.; Roh, B.; Hwang, I.; Kim, H. Corrosion Resistance and Sintering Effect of Carbon Supports in Polymer Electrolyte Membrane Fuel Cells. *Electrochim. Acta* **2009**, *54*, 6515−6521.
(26) O'Hayre, R.; Cha, S.-W.; Colella, W.; Prinz, F. B. *Fuel Cell Fundamentals*; Wiley: New York, 2006.
(27) Brandes, E. A.; Brook, G. B. *Smithells Metals Reference Book*, 7th ed.; Butterworth Heinemann: Oxford, 1998.
(28) Dharmasena, K. P.; Wadley, H. N. G. Electrical Conductivity of Open-Cell Metal Foams. *J. Mater. Res.* **2002**, *17* (3), 625−631.
(29) Li, Y.; Fu, Z.-Y.; Su, B.-L. Hierarchically Structured Porous Materials for Energy Conversion and Storage. *Adv. Funct. Mater.* **2012**, *22*, 4634−4667.